Available online at www.sciencedirect.com

ScienceDirect

journal homepage: www.elsevier.com/locate/he

Kinetics and mechanism of MgH_2 hydrolysis in $MgCl_2$ solutions

Vasyl Berezovets [a], *Andriy Kytsya* [a,**], *Ihor Zavaliy* [a], *Volodymyr A. Yartys* [b,*]

[a] *Karpenko Physico-Mechanical Institute NAS of Ukraine, 5 Naukova Str., Lviv, 79060, Ukraine*
[b] *Institute for Energy Technology, P.O. Box 40, N-2027, Kjeller, Norway*

HIGHLIGHTS

- Effective hydrolysis of magnesium hydride by adding magnesium chloride.
- Influence of magnesium chloride on the kinetics of the hydrolysis reaction and the yield of hydrogen.
- The effect of magnesium chloride concentration on the passivation layer of magnesium hydroxide.
- Kinetic model of magnesium hydride hydrolysis reaction in the presence of chloride ion.
- Determination of optimal concentrations of magnesium chloride.

GRAPHICAL ABSTRACT

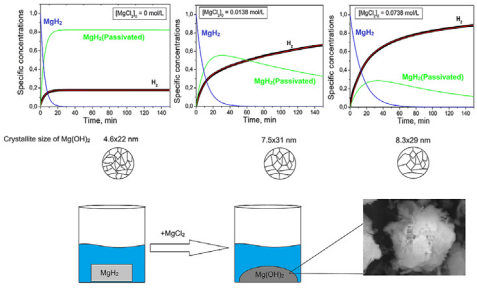

ARTICLE INFO

Article history:
Received 20 March 2021
Received in revised form
22 September 2021
Accepted 28 September 2021
Available online 28 October 2021

Keywords:
Hydrolysis
Magnesium hydride
Magnesium chloride

ABSTRACT

In the present work we systematically studied the hydrolysis of magnesium hydride in $MgCl_2$ aqueous solutions, which was used as a process promotor. The initial hydrolysis rate, the pH of the reaction mixture, and the overall reaction yield are all found to be linearly dependent of the logarithm of $MgCl_2$ concentration. The phase-structural and elemental compositions of the formed precipitates showed that they do not contain chlorine ions and solely consist of $Mg(OH)_2$. The size of the $Mg(OH)_2$ crystallites increased with increasing content of $MgCl_2$ in the aqueous solution.

The best agreement between the observed and modelled hydrolysis kinetics was achieved by applying a pseudo-homogeneous model that describes the process rate as increasing with H^+ ions concentration. The deposition of $Mg(OH)_2$ which is impermeable to water and blocks the surface of the remaining MgH_2 however simultaneously and partially suspends this reaction. We therefore propose a mechanism of MgH_2 hydrolysis in the presence of $MgCl_2$ that is based on the comparison of the kinetic dependencies, variations

* *Corresponding author.*
** *Corresponding author.* Department of Physical Chemistry of Fossil Fuels of the Institute of Physical-Organic Chemistry and Coal Chemistry named after L.M. Lytvynenko of the National Academy of Sciences of Ukraine, 3a Naukova Str., Lviv, 79060, Ukraine.
E-mail addresses: andriy_kytsya@yahoo.com (A. Kytsya), zavaliy@ipm.lviv.ua (I. Zavaliy), volodymyr.yartys@ife.no (V.A. Yartys).
https://doi.org/10.1016/j.ijhydene.2021.09.249
0360-3199/© 2021 The Author(s). Published by Elsevier Ltd on behalf of Hydrogen Energy Publications LLC. This is an open access article under the CC BY license (http://creativecommons.org/licenses/by/4.0/).

of solutions pH and the structural and elemental analysis data for the solid deposits formed during the interaction. We furthermore define the kinetic model of the process, and the equation that describes the variation in pH of solutions containing chloride salts. Hydrolysis efficiency increased with increased relative $MgCl_2$ amount; the best performance being achieved for the stoichiometric ratio MgH_2+0.7$MgCl_2$ ($MgCl_2$/MgH_2 weight ratio of 12.75/100). This provided a hydrogen yield of 1025 mL (H_2)/g MgH_2. Maximum hydrogen yield peaked at 89% of the theoretical H_2 generation capacity, and was achieved within 150 min of hydrolysis start, 35% of hydrogen being released in the first 10 min after start, the hydrogen generation rate being as high as 800 mL $min^{-1} \cdot g^{-1}$ MgH_2.

© 2021 The Author(s). Published by Elsevier Ltd on behalf of Hydrogen Energy Publications LLC. This is an open access article under the CC BY license (http://creativecommons.org/licenses/by/4.0/).

Introduction

The roots of the recent development of hydrogen energy technology lie in the technology's environmental friendliness and efficiency, making it well suited for nonpolluting autonomous and mobile energy storage and generation systems [1–3]. This includes the development of portable energy supply systems that use hydrogen to power fuel cells [4]. The hydrolysis of various compounds in aqueous solutions is considered as an important route to on-site hydrogen generation. Borohydrides of alkali metals [5,6], magnesium [7] and aluminum [8] metals and their alloys [9,10] and corresponding metal hydrides are considered as the most efficient materials for chemical hydrogen generation.

The current focus in hydrolysis process research is on increasing the efficiency of use of Mg hydride [11]. The hydrolysis of magnesium hydride, despite the $MgH_2 + 2H_2O = Mg(OH)_2 + 2H_2$ ($\Delta G^0_{298} = -323$ kJ/mol) [12] reaction's high thermodynamic driving force, unfortunately stops after just appr. 20 min of interaction at its low conversion level of ~20% due to the formation of a passivating $Mg(OH)_2$ layer covering the surface of MgH_2 [12,13].

Different additives have been utilized to overcome the passivation process challenges, both organic [12,14] and inorganic acids [7,13] appearing to be the most efficient additives for promoting the hydrolysis and serving as protons donors [14,15]. As the acids add extra weight, the overall hydrogen generation capacity therefore is lower, how much lower depending on the molecular mass of the acid used.

Many studies of the effects of various salts on the hydrolysis of magnesium hydride have been published. These include processes that involve normal [16–18] and acidic [7,18] salts solutions, and the hydrolysis of MgH_2-salt composites [19–21] using deionised/tap/sea water. Additions of various metal chloride salts increase both the hydrolysis yield of MgH_2 and the rate of the process. Different chlorides were in focus of these studies [16,17,19–25], the hydrolysis mechanism appearing to be common for all the studied chlorides where deionised water was used, irrespective of whether their aqueous solutions or composites were used. The most significant alterations of the rates of hydrolysis were, however, found to be related to the pH of the solutions [7].

Maximum conversion and the highest rates of hydrogen generation in hydrolysis of MgH_2 are expected to be achieved by using solutions of acidic salts [7,19]. Increasing the salt content in the solution or in the composite increases hydrogen yield, this reaching a maximum at the optimum salt content before declining. The NH_4Cl (0.5 mol/L) solution is particularly efficient, allowing almost the complete conversion of MgH_2 and quickly yielding 1683 mL (H_2)/g MgH_2, probably due to the elimination of the $Mg(OH)_2$ formation [26].

The different salts of hydrochloric acid are additives that efficiently accelerate the MgH_2 hydrolysis process. The salts formed by weak alkalis (NH_4^+ [27], Mg^{2+} [20,22,23,28], Zn^{2+}, Fe^{3+}, Zr^{4+} [20]) and hydrochloric acid HCl (a strong acid) are also among the strongest promoting additives. Our choice of magnesium chloride as an additive was based on the available reference data which documented its superior effect as compared to the other studied metal chloride salts on the rates of the hydrolysis of MgH_2 and on the completeness of the process while at the same time $MgCl_2$ is a cost-efficient material. The hydrolysis of MgH_2 in aqueous solutions of $MgCl_2$ has been studied in [18,19,22–24]. The properties of the different types of MgH_2 powders used in the studies, however, varied. This conclusion stands despite these property variations clearly influencing the specific interaction features. A hydrogen yield of 1635 mL/g [23] and 1137 mL/g [22] using, respectively, 0.5 mol/L and 0.05 mol/L solutions of $MgCl_2$ after 50 [23] and 90 [22] minutes of interaction, was achieved.

A composite of MgH_2 and $MgCl_2$ was prepared in [19] by milling their mixture in a planetary mill. Milling was accompanied by an increase in the specific surface area (several times over); no dependence, however, established between milling time and specific surface area. Hydrogen yield also does not seem to be directly related to milling time. The temperature of interaction does, however, affect hydrolysis behavior. $MgCl_2$ undergoes exothermic dissolution in water, the released heat therefore increasing the temperature and affecting the efficiency of the MgH_2 conversion. These features all affect the overall hydrolysis behavior of MgH_2. The reference point, when comparing the properties of the MgH_2–$MgCl_2$ systems, could be the data obtained for the milled for 30 min mixture MgH_2–3 mol % $MgCl_2$, the period in which the most pronounced improvement in hydrolysis behavior was observed. Such a mixture provided a hydrogen yield of

964 mL/g. Thus, magnesium chloride may be considered as a perspective material to improve the efficiency of the hydrolysis of magnesium hydride as it is ecofriendly, is affordably priced and has a low molecular mass (which defines the overall hydrogen generation efficiency of the MgH_2+$MgCl_2$ mixtures).

The chemical interactions mechanisms in the MgH_2–MCl_n–H_2O systems in general and in the system MgH_2–$MgCl_2$–H_2O in particular have, unfortunately, not been sufficiently well studied. It can, however, be assumed that the hydrolysis of magnesium hydride in the presence of metal chlorides is facilitated due to hydrolysis of salts resulting in a hydrochloric acid formation (Reaction I.1). This is supported by the experimental data [20].

$$MCl_n + nH_2O \Leftrightarrow M(OH)_n + nHCl \quad (I.1)$$

$$2HCl + MgH_2 = MgCl_2 + 2H_2 \quad (I.2)$$

The amounts of metal chlorides used in Ref. [20] are significantly smaller than the amount of magnesium hydride involved in the process. According to the Reaction I.2, the amount of hydrochloric acid formed is insufficient to allow a complete conversion of MgH_2.

In general, it is known that the rate of the hydrolysis increases with growing acidity of the solutions. On the other hand, pH of the solutions of the chloride salts strongly depends on the type and concentration of the cations in the solutions and changes in a broad range between pH > 1 and < 7, as it is shown in Fig. 1. Most importantly, the conversion rate of the hydrolysis of MgH_2 increases following a decrease in the pH of the solution, in a sequence $ZnCl_2$<-$AlCl_3$<$FeCl_3$<$ZrCl_4$, as shown in Fig. 1. Fig. 1 clearly shows that the conversion extent of magnesium hydride increases with increasing acidity of the solutions occurring because of the formation of the corresponding metal hydroxides. Thus, a more significant extent of the hydrolysis of the metal salts causes the formation of higher amounts of hydrochloric acid, see the Reaction I.2.

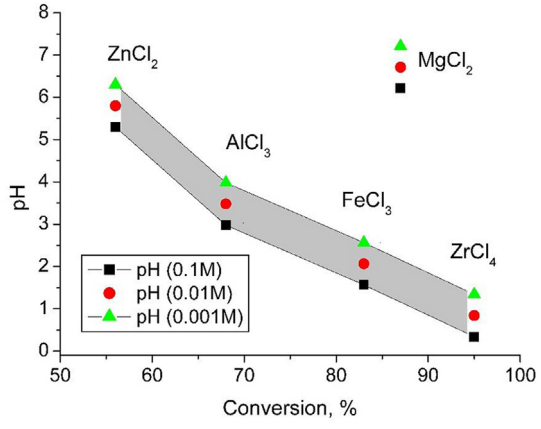

Fig. 1 – Dependence of the maximal conversion rate of MgH_2 [20] on the pH of their chloride solutions (calculated in this study for the different concentrations of the chloride solutions, 0.001–0.1 M) showing an increasing progression of the hydrolysis process following a decrease of the pH of the solutions in a sequence $ZnCl_2$<$AlCl_3$<$FeCl_3$<$ZrCl_4$. An unusual behavior of $MgCl_2$ is evident as a high conversion rate of MgH_2 does not correlate with a relatively high pH of the solutions of $MgCl_2$.

Many aspects relevant to the description of the catalytic and promoting behaviors of the metal chlorides, however, remain unclear. This includes a significant catalyzing effect which demonstrates $MgCl_2$ on the hydrolysis process. Interestingly, in spite the corresponding values of the pH for the solutions of $MgCl_2$ show a formation of close-to-neutral solutions (see Fig. 1), the extent of the conversion process appears to be unexpectedly high. Thus, the behavior of $MgCl_2$ significantly deviates from the described trend and deserves to be thoroughly investigated.

Our goal was to study such unusual promoting influence of $MgCl_2$ on the mechanism and kinetics of transformations during the hydrolysis of MgH_2 in $MgCl_2$ solutions.

When studying the effect of $MgCl_2$ we furthermore were motivated by the following arguments:

a) We avoided influence of any other than Mg^{2+} cation on the chemistry of the studied process;
b) $MgCl_2$ is a convenient choice of additive from the applied perspective as it is cost-efficient and safe in use;
c) Mg-containing products of the hydrolysis can be used for the recycling of magnesium without a need for the purification of these products.

The goal of this work was therefore to address the lack of the available data and understanding of the process, by studying the dependence of H_2 evolution during the hydrolysis of MgH_2 from the concentration of $MgCl_2$ aqueous solutions. Using $MgCl_2$ solutions instead of solid $MgCl_2$ as additives allowed to eliminate the effect of exothermic process of dry magnesium chloride dissolution on the studied interaction. The mechanism and the kinetics model of the hydrolysis process of MgH_2 in water solutions were proposed and successfully described the experimental data.

Experimental details

Materials

Magnesium hydride - MgH_2 - was prepared by reactive ball milling of magnesium (Fluka, grit, 50–150 mesh, 99.8%) in hydrogen gas using a Fritsch Pulverisette-6 planetary ball mill. Milling was carried out in a custom-made SS vial with a volume of 550 mL. The vial was equipped with two Swagelok needle valves for hydrogen inlet and outlet. 50 stainless steel balls (d = 16 mm; m = 817 g) were used as grinding bodies. The weight ratio of the grinding bodies to the weight of the sample was 40:1, grinding being performed at 6.667 Hz (400 rpm) and an initial hydrogen pressure of 2.5 MPa.

Milling was periodically stopped (every 15–20 min) to cool the vial to the room temperature, and to control the mechanochemical hydrogenation process. The vial was then connected to a Sieverts-type apparatus, and the hydrogen pressure was measured using a pressure sensor (measurements

accuracy 0.05%). Hydrogen gas was, following this, reintroduced into the vessel until the initial pressure of 2.5 MPa was reached, and the milling process then being continued. The amount of hydrogen absorbed by the sample in the reactive ball milling process was determined using the volumetric method, by measuring pressure changes in a calibrated volume. Magnesium hydride was, after grinding, unloaded from the vial in the glove box filled with a purified argon gas.

Magnesium chloride ($MgCl_2 \times 6H_2O$, 99%) and citric acid ($C_6H_8O_7 \times H_2O$, 99%) were acquired from commercial suppliers and were used as received.

Hydrolysis studies and pH measurements

Kinetics of MgH_2 hydrolysis was investigated at 20 °C in pseudo-isothermal conditions, in a setup similar to that described in [23]. This consisted of a two-neck glass vessel immersed in a water bath equipped with a magnetic stirrer and injectors for the $MgCl_2$ solutions and citric acid. 0.2 g of MgH_2 was typically introduced into the reactor, 20 mL of an aqueous solution prepared using deionised water (pH = 7.00) being quickly added. The generated hydrogen was released through Allihn-type fluid-cooled condenser connected to a bottle filled with water, at room temperature, the H_2 then being collected by replacing the water in a beaker. The citric acid solution (2 mol/L; 20 mL) was introduced after the hydrolysis reaction slowed down, to measure the amount of unreacted MgH_2 and to evaluate the extent of MgH_2 conversion. This resulted in a complete dissolution of the solid components - $Mg(OH)_2$ and MgH_2, formation of a transparent solution and release of the remaining in unreacted MgH_2 hydrogen gas. In total, when summing up the amounts of the originally formed H_2 and hydrogen released by interaction with citric acid, a completeness of the hydrolysis of MgH_2 was confirmed.

The pH of the reaction mixtures was monitored 100 min after the start of the hydrolysis experiment, using a pH electrode that was carefully calibrated prior to measurements. Standard buffer solutions having pH = 7.00, pH = 9.21, and pH = 11.00 were used.

XRD studies and elemental analysis

The solid products of the hydrolysis experiments used in the XRD analysis were obtained without the addition of the citric acid. The prepared slurries were filtered and washed with a distilled water, the XRD patterns of these samples being immediately measured at a DRON-3.0 diffractometer using Cu-K_α radiation, to prevent crystallization of the products and/or possible CO_2 induced precipitate hardening. A Pseudo-Voigt function was used in the GSAS [29] Rietveld refinements, which allowed crystallite sizes to be estimated. The instrumental contribution to the broadening of the diffraction peaks was determined from the refinements using LaB_6 as a standard. Crystallite sizes were defined assuming uniaxial broadening, a preferred orientation in the [0,0,1] direction and two size parameters for the prismatic crystallites, one in the [0,0,1] direction and other in a perpendicular plane [30]. Elemental analysis of the precipitates was performed using an EVO-40 XVP (Carl Zeiss) scanning electron microscope equipped with Inca Energy 350 (Oxford Instruments) microprobe analysis system.

Table 1 – Composition of the studied samples $MgH_2 + MgCl_2$ and conversion rates during the hydrolysis experiments.

Sample No.	Mass ratio $MgCl_2$/MgH_2	C($MgCl_2$), mol/L	Mole ratio $MgCl_2$/MgH_2,	Conversion after 150 min, %
1	0/100	0	0/100	18
2	4.2/100	0.0046	1.2/100	43
3	8.5/100	0.0092	2.3/100	57
4	12.7/100	0.0138	3.4/100	67
5	17/100	0.0184	4.6/100	70
6	35/100	0.0368	9.6/100	79
7	70/100	0.0738	19/100	89

Results and discussion

General features of the hydrolysis process

MgH_2 was, as described earlier, prepared by a reactive ball milling of magnesium in hydrogen gas. The milling lasted for 11 h and resulted in a nearly complete (97%) conversion of magnesium metal into magnesium hydride, the measured hydrogen storage capacity being 7.40 wt % H. The MgH_2 sample obtained after milling contained two modifications of nanocrystalline magnesium hydride, namely, α-MgH_2 (~77%, unit cell parameters a = 4.522 (1), c = 3.0201 (8) Å) and a high-pressure metastable γ-MgH_2 (~23%, unit cell parameters a = 4.538 (3), b = 5.420 (4), c = 4.941 (3) Å) (see Supplementary Information (SI) file, Fig. S1). The different thermodynamic stabilities of α-MgH_2 and γ-MgH_2 can, in principle, affect the ability of magnesium dihydride to participate in the hydrolysis processes, in particular because of the influence of MgH_2 sample surface morphology. Thus, the magnesium hydride obtained was annealed under a hydrogen pressure of 1 MPa at a temperature of 200 °C for 1 day, followed by slow cooling. Annealing was carried out at the temperature for the transformation γ-$MgH_2 \rightarrow$ α-MgH_2 of 200 °C [31]. This resulted in a sample that predominantly consisted of the α-MgH_2 modification (see SI, Fig. S2), γ-MgH_2 being a minor part of the sample.

The influence of $MgCl_2$ concentration on the kinetics of MgH_2 hydrolysis has been studied in a broad range of $MgCl_2$/MgH_2 relative ratios (between mole ratios 0/100 and 19/100, as shown in Table 1).

The experiments were repeated at least 3 times and showed a good data convergence, which agreed well with each other, divergences being less than 3%.

Kinetic curves of hydrogen release (Fig. 2a) show that the addition of $MgCl_2$ has a significant positive effect on the extent of MgH_2 conversion, when compared with pure MgH_2 without $MgCl_2$. The hydrolysis kinetics curves show, in each case, an exponentiality and are made of two parts:

(a) Initial fast release of hydrogen for approximately 10 min, the H_2 generation rate reaching 800 mL $min^{-1} \cdot g^{-1}$ MgH_2 at maximum.
(b) Slow ascending H_2-generation for up to 150 min, the amount of hydrogen produced increasing continuously while the rates of hydrogen release are decreasing.

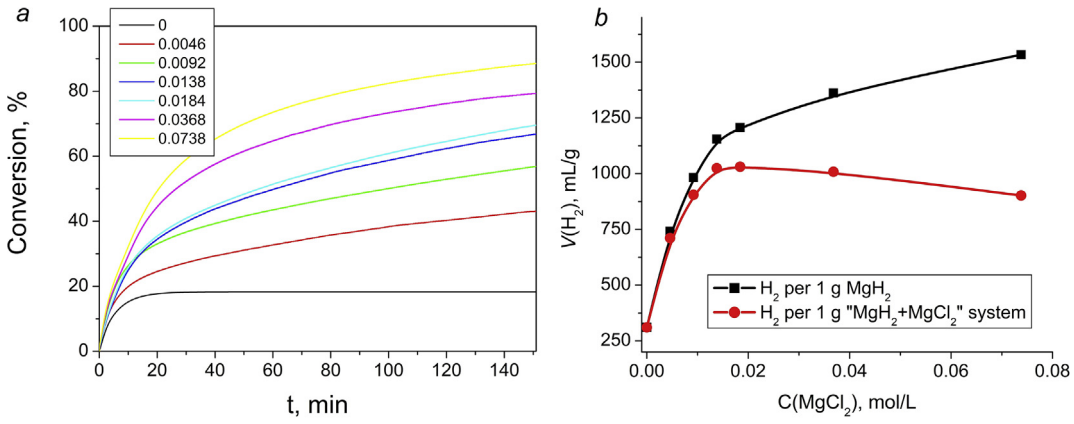

Fig. 2 – Kinetic curves of MgH_2 hydrolysis at different concentrations of $MgCl_2$ (*a*); Dependence of the H_2 generated volume per 1 g of MgH_2 and per 1 g of "MgH_2+$MgCl_2$" system of the molar concentration of $MgCl_2$ (*b*).

Table 2 – Dependence of reaction mixtures pH[a] on $MgCl_2$ concentration.

[$MgCl_2$], mol/L	Weight ratio $MgCl_2/MgH_2$	pH (exp)	pH (calc)
0	0/100	10.89	11.07
0.0092	8.5/100	10.22	10.18
0.0184	17/100	10.10	9.88
0.0368	35/100	9.89	9.58
0.0738	70/100	9.63	9.28

[a] Calculated values of pH (calc) were derived using Equations II.4 i III.7 (see Chapter Acid-base equilibria in the $MgCl_2$ solutions at MgH_2 hydrolysis).

MgH_2 conversion peaked at 89% (see Table 1). Efficiency should however also account for the overall mass of the system, including the $MgCl_2$. Therefore, in Fig. 2b, the hydrogen generation efficiency is given per unit mass of MgH_2 and also per 1 g of the "MgH_2+$MgCl_2$" mixture used.

It can be concluded from the data in Fig. 2b that the best "MgH_2+$MgCl_2$" system performance was at a $MgCl_2/MgH_2$ weight ratio of 12.75/100 ($C(MgCl_2)$ = 0.0184 M). This gave hydrogen yield of 1025 mL (H_2)/g per 1 g of the "MgH_2+$MgCl_2$" system. Comparison of our data for hydrogen generation at $MgCl_2$ concentrations 0.0184 and 0.0738 M with previously published systems are presented in Table S1 (see SI, Chapter S2). The data of the Table S1 clearly show that for the undoped MgH_2 maximum hydrogen yield does not exceed 26% while the hydrogen generation rate is insufficient for practical applications. In contrast, in the solutions of $MgCl_2$ the performance of MgH_2 in the hydrolysis process becomes superior. This is shown by the current study when the hydrolysis yield reaches 89% for 0.073 M $MgCl_2$ solution while the rates of hydrogen generation are much higher as compared to the process in pure water. The hydrolysis performance for MgH_2 is close to the best characteristics of this studied system observed in the reference data (see the data of the Table S1 and References S1–S14 for further details).

One of the main factors controlling the rate of MgH_2 hydrolysis is the acidity (pH) of the reaction mixtures [12]. It has been earlier reported [20] that the pH of the reaction solutions

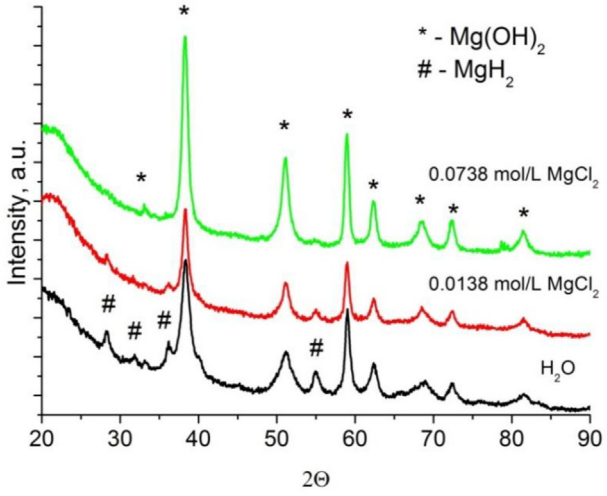

Fig. 3 – XRD patterns of the precipitates obtained at different $MgCl_2$ concentrations.

in the presence of chloride ions is lower than that the pH of the additive-free solutions. pH has also been shown to be dependent on the nature of the chloride salt.

The measurements show that pH decreases with increasing $MgCl_2$ concentration (Table 2). The lowering of pH is explained in [28] by the hydrolysis of $MgCl_2$ salt and the formation of HCl, and the formed hydrochloric acid removes the $Mg(OH)_2$ passivation film from the MgH_2 surface.

A good agreement between the experimental and calculated results is evident from the data presented in Table 2.

Phase-structural composition of the hydrolysis products

Hydrolysis acceleration in the presence of $MgCl_2$ can, as mentioned, be due to the formation of complex solid precipitates that are less soluble than $Mg(OH)_2$, this leading to a decrease in the pH of the solution [20].

Hydrolysis reaction precipitates were studied using XRD and EDS. Analysis of the XRD pattern (Fig. 3) shows that the final products of the reaction contain hexagonal $Mg(OH)_2$

(brucite-type) and unreacted MgH_2. XRD phase-structural analysis showed an increase in the content of $Mg(OH)_2$ which occurred with an increase in the $MgCl_2/MgH_2$ ratios. Furthermore, we observed substantial changes in the characteristics of the crystallites of the formed $Mg(OH)_2$.

The sizes of the $Mg(OH)_2$ crystallites formed (see SI, Chapter S3, Fig. S3-S6) were refined by Rietveld fitting of the XRD pattern, indicating the formation of the $Mg(OH)_2$ nanoflakes. $Mg(OH)_2$ crystallites are formed at the surface of MgH_2 and have a long base of approximately 20–30 nm, irrespective of the Cl^- ions content. Crystallites can be considered to be thin plate-like nanoflakes, thickness (P_{SHORT}) increasing with increasing Cl^- ions concentration and doubling from 4.6 to 8.3 nm (Table 3).

Such a substantial increase of the crystallites sizes shows that in the $MgCl_2$ solutions the number of the $Mg(OH)_2$ nuclei is relatively small while their size becomes larger, when taking into account that $Mg(OH)_2$ content increased by 8% only, from 90.5 to 98.7 wt %. This was accounted when elaborating the mechanism of influence of $MgCl_2$ on the hydrolysis of MgH_2 (see Chapter The mechanism of the influence of $MgCl_2$ on MgH_2 hydrolysis).

Hydrolysis acceleration in presence of $MgCl_2$ can, as mentioned, be related to the formation of complex solid precipitates formed in the $Mg(OH)_2$–$MgCl_2$–H_2O system (which is similar to Sorel cement [32–34]) that are less soluble than $Mg(OH)_2$. This will cause a decrease in the pH of the solution [20].

An isothermal section of the $Mg(OH)_2$–$MgCl_2$–H_2O system at 23 °C is shown in Fig. 4 [34]. The system, as shown by the diagram, contains two pseudoternary solid phases, having compositions 5 $Mg(OH)_2 \cdot MgCl_2 \cdot 8H_2O$ (A) and 3 $Mg(OH)_2 \cdot MgCl_2 \cdot 8H_2O$ (B). These phases are present in the phase diagram shown in Fig. 4.

The formation of any solid phase in the $Mg(OH)_2$–$MgCl_2$–H_2O system [20] is, according to [32], only possible at high $MgCl_2$ concentrations which exceed 1 mol/L.

The concentration limit of $MgCl_2$ solutions was set to 0.0738 mol/L in maximum, that is why the formation of only one solid phase, $Mg(OH)_2$, remained possible. This is in agreement with the phase diagrams presented in [34,35]. During the hydrolysis reaction, the amount of $Mg(OH)_2$ increases while the concentration of $MgCl_2$ remains stable. The equilibrium in the system is shifted towards the formation of magnesium hydroxide while remaining in a "gel" region [34] where the crystallization of $Mg(OH)_2$ occurs. Such a mechanism of interaction is in line with the XRD experimental data.

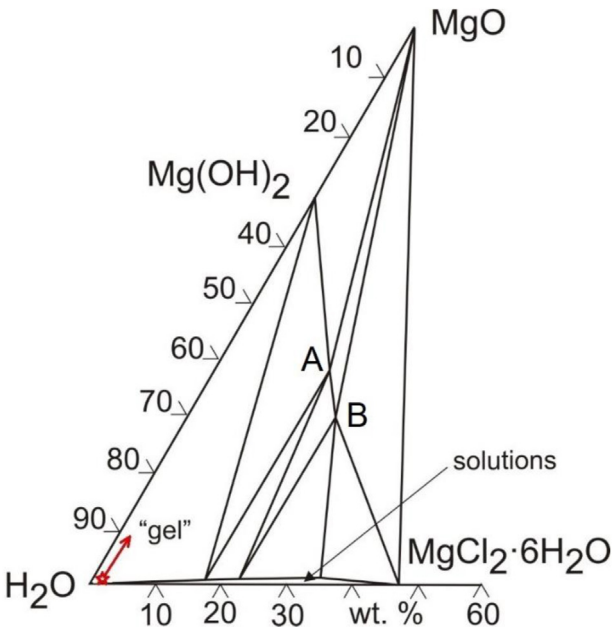

Fig. 4 – Isothermal section of the phase diagram of the system MgO–$MgCl_2$–H_2O [34] at 23 °C.

XRD data agrees well with the elemental analysis results, the precipitates showing an absence of chlorine ions in their composition (see SI, Chapter S3, Table S3). Co-precipitation of a mixed $Mg(OH)_xCl_y$ hydroxochloride appears to be unlikely as, according to [20,36], a solid solution of $Mg(OH)_xCl_y$ ($x + y = 2$) with a crystal structure type of brucite $Mg(OH)_2$ exists in the range $0 < y < 0.3$ and it is only formed by the dehydration of the $xMg(OH)_2 \cdot yMgCl_2 \cdot nH_2O$ phase at temperatures above 205 °C. This is obviously beyond the conditions of the present study. The observed decrease in the pH of the reaction mixture therefore is due to a different origin.

Acid-base equilibria in the $MgCl_2$ solutions at MgH_2 hydrolysis

The mechanism of the process involves a set of physical-chemical reactions that describe an equilibrium being reached in the reaction mixture. The MgH_2–H_2O–$MgCl_2$ system must therefore be considered in detail. The physical-chemical transformations were analyzed using molar concentrations of the components in the reaction mixture (mol/

Table 3 – Results of phase-structural characterization of the precipitates.

[$MgCl_2$], mol/L	Mass ratio $MgCl_2/MgH_2$	MgH_2 content, wt. %	$Mg(OH)_2$ content, wt.%	Refined unit cell parameters of $Mg(OH)_2$, Å	Crystallites size P_{SHORT}, nm	Crystallites size P_{LONG}, nm
0	0/100	9.5 (7)	90.5 (2)	$a = 3.150$ (2) $c = 4.794$ (5)	4.6 (2)	22 (1)
0.0138	12.7/100	6.0 (9)	94.0 (1)	$a = 3.149$ (2) $c = 4.782$ (4)	7.5 (2)	31 (2)
0.0738	70/100	1.3 (3)	98.7 (1)	$a = 3.1479$ (9) $c = 4.781$ (2)	8.3 (3)	29 (1)

L). Possible chemical transformations can therefore be written as follows:

a) Hydrolysis of MgH_2 in pure water

$$MgH_2 + 2H_2O = Mg(OH)_2 + 2H_2\uparrow \quad \text{(II.1)}$$

$$Mg(OH)_2 \Leftrightarrow Mg(OH)_2\downarrow \quad \text{(II.2)}$$

$$Mg(OH)_2 \Leftrightarrow Mg(OH)^+ + OH^- \quad \text{(II.3)}$$

$Mg(OH)_2$ is a weak alkali with a low solubility in water. The basicity constant (pK_1) of freshly precipitated $Mg(OH)_2$ is 2.58 and the value of the solubility product (pSP) is 9.22 [37]. Note that $Mg(OH)_2$ dissociates only partially (Equation II.3). The calculated concentrations of Mg^{2+} and OH^- become equal to $5.3 \cdot 10^{-4}$ and $10.6 \cdot 10^{-4}$ mol/L, respectively, when the $Mg(OH)_2$ precipitate is formed, and with the progressing conversion reaction. The pH of the solution can then be calculated as follows:

$$pH = 14 - \tfrac{1}{2}\, pK_1 + \tfrac{1}{2} \log(C_B) \quad \text{(II.4)}$$

here C_B is the $Mg(OH)_2$ concentration, which can be considered to be equal to the concentration of the dissolved hydroxide, i.e. to $5.3 \cdot 10^{-4}$ mol/L. The calculated pH of the solution of 11.07 is in a good agreement with the experimentally measured pH (see Table 2), thus validating the evaluation.

b) Hydrolysis of MgH_2 in a $MgCl_2$ solution

We can expect the following reactions to occur in $MgCl_2$ solutions:

$$MgCl_2 + H_2O \Leftrightarrow Mg(OH)^+ + H^+ + 2Cl^- \quad \text{(III.1)}$$

$$MgH_2 + 2H^+ = Mg^{2+} + 2H_2\uparrow \quad \text{(III.2)}$$

$$MgH_2 + 2H_2O = Mg(OH)_2 + 2H_2\uparrow \quad \text{(III.3)}$$

$$Mg(OH)_2 \Leftrightarrow Mg(OH)_2\downarrow \quad \text{(III.4)}$$

$$Mg(OH)_2 \Leftrightarrow Mg(OH)^+ + OH^- \quad \text{(III.5)}$$

The reaction solution is, as can see be seen, acidic before the introduction of MgH_2. The pH of such a solution can be calculated using an equation,

$$pH = 7 - \tfrac{1}{2}\, pK_1/2 \; - \; \log([MgCl_2]) \quad \text{(III.6)}$$

where the concentration of $MgCl_2$ in mol/L is denoted as $[MgCl_2]$.

The pH of the initial $MgCl_2$ solutions are in the range 6.28–6.88 under the applied experimental conditions, and are therefore close to neutral. The onset of the hydrolysis reaction and the formation of $Mg(OH)_2$ take place after adding the MgH_2, the magnesium hydroxide precipitates are forming after some time. The reaction system therefore appears to contain two solid species, MgH_2 and $Mg(OH)_2$, which are in equilibrium with the solution, stable concentrations of the soluble species - $Mg(OH)_2$ and $MgCl_2$ – therefore continuing.

Such a $MgCl_2 + Mg(OH)_2$ solution can be considered as a buffer solution "weak base and its salt with a strong acid". The pH of such a solution can be calculated by using the equation:

$$pH = 14 - pK_1 + \log([Mg(OH)_2]/[MgCl_2]) \quad \text{(III.7)}$$

Magnesium hydroxide has, as mentioned, low solubility in water. The concentration of $Mg(OH)_2$ in the solution, after precipitation, will therefore be constant and can be calculated using pSP. Reaction mixture pH should therefore be linearly dependent on log ($[MgCl_2]$), an assumption that is in good agreement with experimental observations, see Fig. 5a.

Fig. 5b shows excellent agreement between pH calculated using the Equation II.4 (hydrolysis of MgH_2 in water) and Equation III.7 (hydrolysis of MgH_2 in aqueous solutions of $MgCl_2$) and experimentally measured pH values. The correlation coefficient is 0.98. We can, based on this, therefore conclude that there is a linear dependence between the convention rate of the hydrolysis of MgH_2 and log ($[MgCl_2]$), see Fig. 5c.

Some differences between the experimentally measured pH as compared to the pH (calc) (Table 2) may be related to the $Mg(OH)_2$ concentration in a real system being higher than the concentration calculated using pSP. This is due to the fact that precipitation of magnesium hydroxide requires the supersaturation of the solution [38].

The mechanism of the influence of $MgCl_2$ on MgH_2 hydrolysis

In Chapter Acid-base equilibria in the $MgCl_2$ solutions at MgH_2 hydrolysis. we described the chemical transformations that take place in reaction mixtures containing $MgCl_2$ and presented the equations suitable for successfully predicting solution pH, based on calculation results agreeing with the experimental data. The mechanism of the physical-chemical transformations during the MgH_2 hydrolysis is, however, still not known. This Chapter therefore focuses on achieving a better understanding of the processes that take place during the crystallization of $Mg(OH)_2$, including the formation of a passivation film on the surface of MgH_2. Classical Nucleation Theory (CNT) has been used to describe the studied process in this study.

The processes of $Mg(OH)_2$ crystallization and MgH_2 passivation start in the reaction mixture immediately after component mixing. These continue until the hydrolysis process is finished. The morphology of the passivating film and its permeability to water are defined at the initial stage of $Mg(OH)_2$ crystallization. Both these features are very important, as they directly influence the overall conversion level and the hydrogen gas yield.

The initial rate of the process is very high for the MgH_2 hydrolysis studied, which makes direct experimental observations difficult.

We therefore considered the following modeling description of the system:

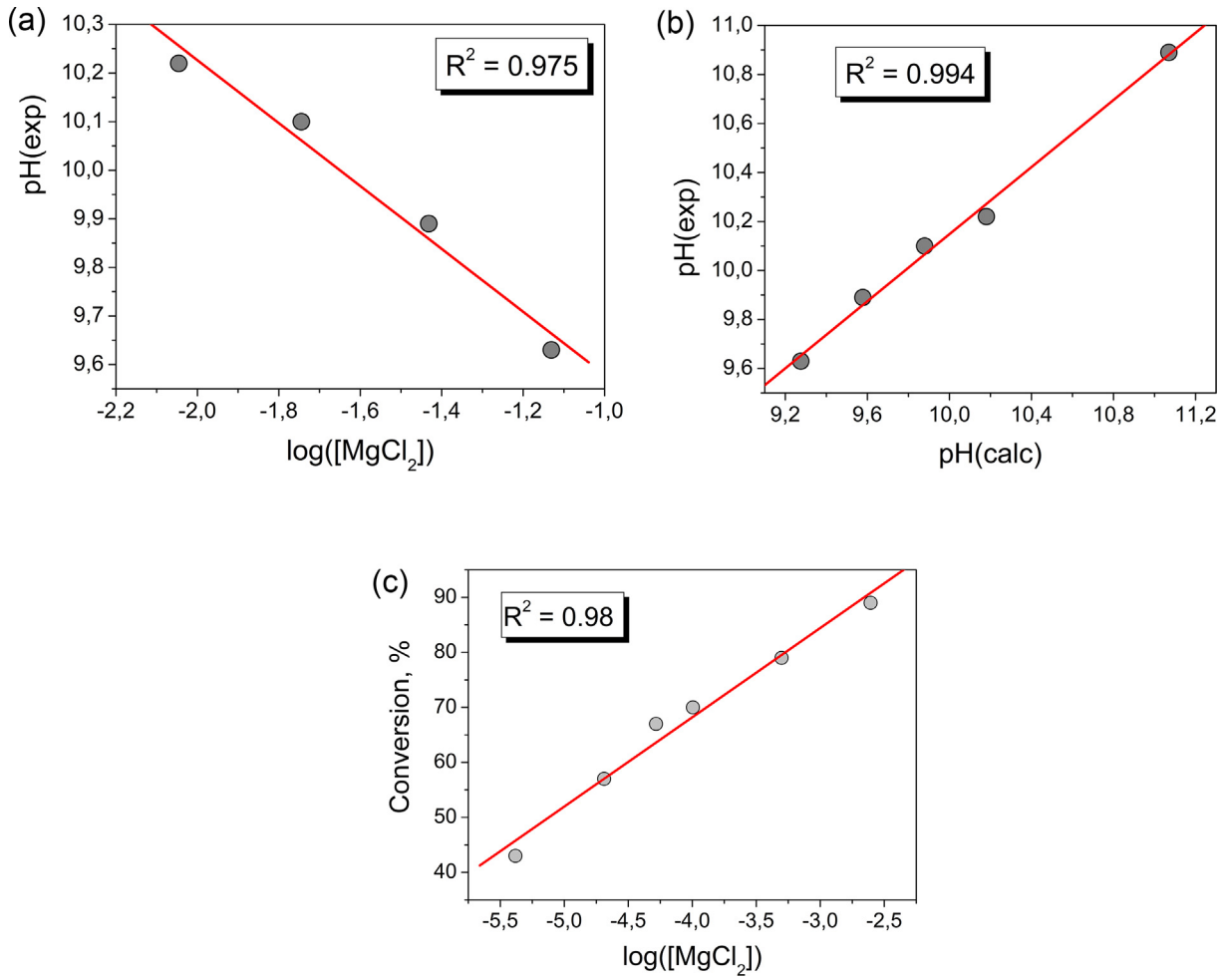

Fig. 5 – Dependence of the working solution pH on the logarithm of $MgCl_2$ concentration (*a*), correlation between calculated and experimentally measured values of pH (*b*), and dependence of the conversion rate at 150 min on log ([$MgCl_2$]) (*c*).

1) We calculated, using Equations II.4 and II.7, the pH of the reaction mixtures in relation to the transformation extent of MgH_2 in the process starting period (Fig. 6).

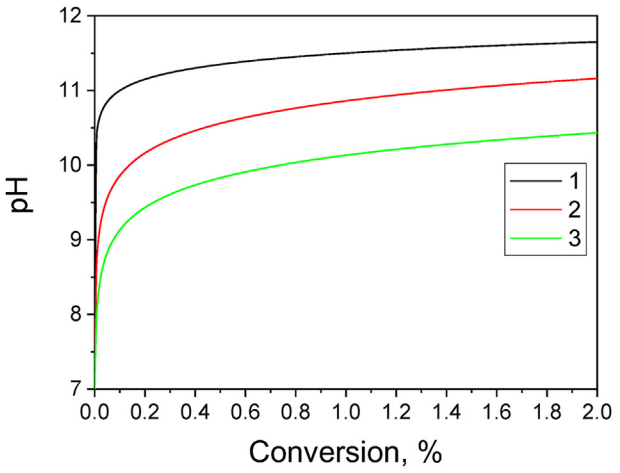

Fig. 6 – Changes of solutions pH during MgH_2 hydrolysis in pure water (1) and in the $MgCl_2$ aqueous solutions, 0.0138 (2) and 0.0738 (3) mol/L, respectively.

The behaviors of the system are, as clearly shown by Fig. 6, distinctly different where $MgCl_2$ is present or absent in the solutions, and at varying concentrations. An abrupt increase in pH occurs in pure water, pH quickly reaching 11.5. The addition of $MgCl_2$ and increasing its concentration, therefore clearly and significantly decrease the pH of the solution, making its variations slower.

2) We can, using CNT [39], define the size of a critical nuclei of an emerging new phase of $Mg(OH)_2$ via the following equation:

$$r(cr) = \frac{2V_m\sigma}{RT\ln(C_{cr}/C_\infty)} \quad \text{(IV.1)}$$

where σ is surface tension, V_m is the molar volume of the solid phase formed, R is a molar gas constant, T is temperature, C_∞ is an equilibrium concentration of $Mg(OH)_2$ in the solution (concentration of a saturated solution above the macrophase with a flat surface) and C_{cr} is a critical concentration at which a nucleation of new centers of the crystallization occurs.

Equation IV.1 clearly demonstrates that the size of the critical nuclei is defined by the coefficient of supersaturation

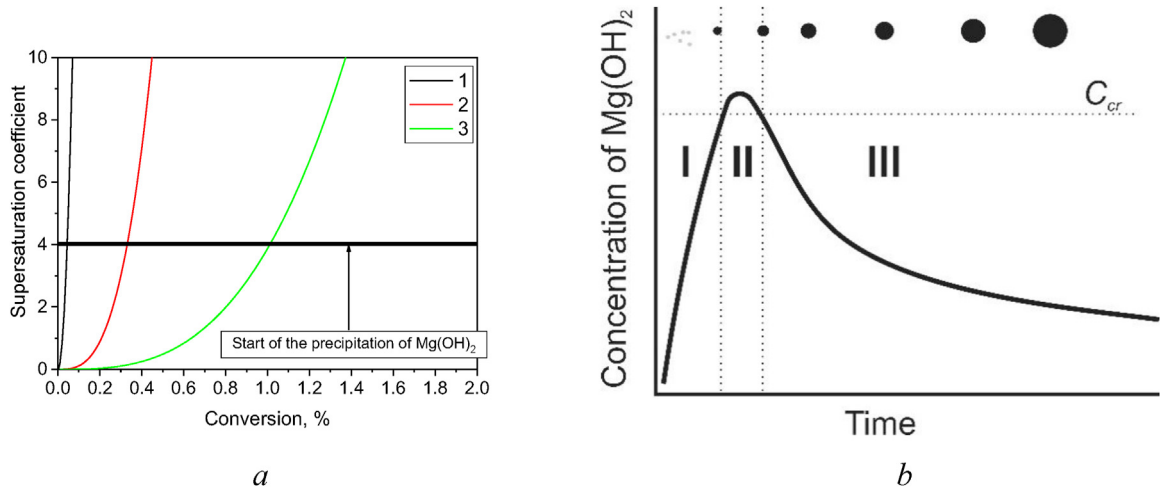

Fig. 7 – Dependencies of the supersaturation coefficient on the hydrolysis conversion rate in pure water (1) and in the $MgCl_2$ solutions (2–0.0138 mol/L and 3–0.0738 mol/L $MgCl_2$) (*a*); time dependence of $Mg(OH)_2$ concentration changes based on the general model approach presented in Ref. [40] (*b*). Step I: solution of $Mg(OH)_2$; Step II: nucleation of $Mg(OH)_2$ precipitates; Step III: growth of $Mg(OH)_2$ precipitates. The overall process is described in detail later in the paper.

(C_{cr}/C_∞). C_∞ will therefore, in this case, be defined by the solubility of a freshly precipitated $Mg(OH)_2$, which is $5.3 \cdot 10^{-4}$ mol/L (pSP($Mg(OH)_2$) = 9.22). The value of C_{cr} for the system $Mg(OH)_2$–$MgCl_2$–H_2O is unknown, reference data being however available [38]. This data states that the smallest value for the coefficient of supersaturation that is required for $Mg(OH)_2$ deposition is $C_{cr}/C_\infty = 4$. The current concentration [$Mg(OH)_2$] can be calculated from the extent of MgH_2 conversion. We therefore simulated changes in the coefficient of supersaturation in relation to the extent of conversion reaction, and presented the dependencies in Fig. 7.

It is clear from Fig. 7a that crystallization and, correspondingly, the formation of the passivating surface layer during MgH_2 hydrolysis in water, starts even at a very low conversion level of MgH_2 of 0.04%. This formation occurs, however, in the $MgCl_2$ solutions at significantly higher MgH_2 conversion levels of 0.3 and 1% for solutions containing 0.0138 and 0.0738 mol/L $MgCl_2$, correspondingly.

3) Equation IV.1, as mentioned, describes the thermodynamics of the phase transformation, but is not applicable to the evaluation of the rates of the changes for system component content. The model proposed in Ref. [40] is, however, well suited to the description of the kinetics of the new solid phase formation process during its crystallization from the solution.

The following physical chemical process steps, based on this model and as shown in Fig. 7b, take place during new phase nucleation, leading to the formation of the $Mg(OH)_2$ precipitates:

(I) Increase in the content of magnesium hydroxide dissolved in the solution, formed during the MgH_2 hydrolysis process in the solution, until reaching its critical concentration C_{cr}, which is required to initiate solid precipitate nucleation;

II) Fast crystallite nucleation process leading to a decrease in the $Mg(OH)_2$ content of the solution;

III) Concentration of $Mg(OH)_2$ in the solution decreasing after nucleation starts, and new particle crystallization terminating. Growth of the already formed particles, however, proceeds via a diffusion controlled deposition of $Mg(OH)_2$ on the surface of the available particles.

The kinetics curve showing the three individual steps I-II-III, Fig. 7b, can be successfully described using the following system of Equations IV.2 as proposed in Ref. [41]:

$$\frac{dC}{dt} = Q - j \cdot n - G \cdot P$$
$$\frac{dP}{dt} = j \qquad \text{(IV.2)}$$

where Q is the rate of compound supply into the reaction zone, j is the nucleation rate, n is the size of the critical nucleus, G is the rate of particle growth, and P is concentration of the particles.

The use of these equations in the $Mg(OH)_2$ deposition case studied is, however, complicated by the high rate of MgH_2 hydrolysis in the initial stage of the process, even where pure water is used instead of the $MgCl_2$ solution. Where pure water is used, the supersaturation coefficient threshold value required for $Mg(OH)_2$ deposition is reached instantaneously, immediately after contact between the water and MgH_2 (see Fig. 7 for the details). Fluctuations in $Mg(OH)_2$ concentration is another factor that complicates the modeling process. These difficulties can, however, be overcome by using CNT with the presented kinetic modeling approaches, this allowing the observed regularities to be successfully described. This is, however, at a qualitative level rather than through a quantitative agreement between the modeling results and the experiment.

The following are the arguments that validate our proposed approach.

a) The product of Mg^{2+} and OH^- concentrations quickly increases without $MgCl_2$ present in the solution, allowing high rates of reactant supply into a zone of interaction. This is quantified by the parameter Q, see Equation IV.2, causing a quick increase in the supersaturation coefficient for magnesium hydroxide (see Fig. 7a). This quick increase in the reaction zone leads to high C_{cr}/C_∞ values in the system, for a prolonged period of time. The new phase nucleation process (Process II in Fig. 7b) therefore becomes quite lengthy, causing the formation of a large number of individual $Mg(OH)_2$ nuclei.
b) The use of $MgCl_2$ solutions in the hydrolysis process causes the formation of a buffer solution, its pH being defined by Equation III.7. The product of Mg^{2+} and OH^- ion concentrations increases much more slowly, causing a decrease in the reactant supply rate, Q. This in turn causes a lower rate of C_{cr}/C_∞ increase (see Fig. 7a), the C_{cr}/C_∞ value required for the formation of a critical nuclei also being more slowly reached. Further supply of the reactants into the zone of interaction drops in relation to the previously described case of pure water. Stage II duration (Fig. 7b) therefore becomes shorter, this also decreasing the number of nucleated new phase particles.

A high rate of reactant supply to the zone of interaction, as in the hydrolysis of MgH_2 in water, furthermore allows higher values of C_{cr}/C_∞ to be reached than for the hydrolysis performed in the $MgCl_2$ solutions. This also, according to Equation IV.2, leads to a decrease in the size of crystal nuclei.

The model approach that has been presented therefore allows the differences in behaviors during MgH_2 hydrolysis in pure water and in the $MgCl_2$ solutions to be explained. In pure water, the nucleation of a large number of small sized particles takes place at the very start of the hydrolysis process. In the $MgCl_2$ solutions, however, the number of $Mg(OH)_2$ nuclei is smaller, but their sizes are larger. An increase in the concentration of $MgCl_2$ further causes a growth in $Mg(OH)_2$ crystallite sizes, from 4.6 nm in water to 8.3 nm in the $MgCl_2$ solutions. This causes an inhomogeneous film of hydroxide to form on the surface of MgH_2.

The $MgCl_2$ action mechanism in the MgH_2 hydrolysis reaction can, based on the above experimental data and modeling, be described as follows. The MgH_2 and water reaction, which forms soluble $Mg(OH)_2$, is suggested as being a very fast process due to the minor influence of this on the pH of the starting reaction mixture in initial $MgCl_2$ solution hydrolysis:

$$MgH_2 + 2H_2O = Mg(OH)_2 + 2H_2\uparrow$$

Such a reaction leads to the formation of a buffer solution $MgCl_2 + Mg(OH)_2$ ("weak base – its salt with a strong acid") that determines the pH of the reactive solution. The pH of such a solution increases with increasing conversion (causing increased $Mg(OH)_2$ concentration) up to the solubility product of magnesium hydroxide being reached, at which point precipitation of $Mg(OH)_2$ starts. The concentration of $Mg(OH)_2$ in the solution, after precipitation begins, remains constant and pH remains stable (Equation III.7).

It should finally be noted that the product of $[Mg^{2+}] \times [OH^-]^2$ concentrations dramatically decreases in the presence of $MgCl_2$, and that this is the reason for the decreased rate of the new phase ($Mg(OH)_2$) formation and the increased size of the nuclei, which leads to

1) the formation of an inhomogeneous passivation film, causing improved water access to the MgH_2 surface

and

2) the increase of $Mg(OH)_2$ precipitate crystallinity, leading to the lowering of their solubility, to the re-crystallization of $Mg(OH)_2$ (due to the mass transfer from smaller $Mg(OH)_2$ clusters to larger ones) and an increased passivation film inhomogeneity.

One additional aspect of the hydrolysis process also deserves to be mentioned. The pH of the reaction mixture is, as noted, determined by the $MgCl_2$ concentration. Full hydrolysis can occur when a different type of chloride salt than $MgCl_2$ is used (for example $FeCl_3$, $ZrCl_4$). This can be due to the formation of the insoluble hydroxide, the metal cations being excluded from the reaction mixture because of the formation of $Fe(OH)_3$ or $Zr(OH)_4$. The resulting solution therefore contains only OH^-, Cl^-, and Mg^{2+} ions, which leads to the formation of a buffer solution. The pH of the reaction mixture can be evaluated by Equation III.7, which is similar to the case of adding $MgCl_2$.

This means that the overall conversion of MgH_2 by the hydrolysis reaction is primarily dependent on the concentration of chlorine anions. The nature of the cations will influence the reaction rate, resulting in a complete precipitation of the corresponding metal hydroxide.

The addition of salts which are not subject to the hydrolysis process (for example, NaCl), in contrast does not influence the reaction process, as the resulting solution consists of OH^-, Cl^-, Mg^{2+}, and Na^+. The negatively charged chlorine anions in the reaction system will be compensated by Na^+, but not by Mg^{2+}. A buffer solution will therefore not be formed, and the pH will be determined by Equation II.4.

Kinetic model of MgH_2 hydrolysis in the presence of Cl^- anions

The kinetics of the MgH_2 hydrolysis is frequently described using the Avrami-Erofeev Equation V.1 [11,27,42].

$$\alpha(t) = 1 - \exp\{-kt^n\} \quad (V.1)$$

where $\alpha(t)$ is the hydrogen generation rate in the MgH_2–$MgCl_2$–H_2O system at reaction time t; k is a reaction constant; n is the Avrami constant.

The n value changes can, for the nucleation and growth mechanism, be related to the rate controlling steps of the process, including changes in diffusion dimensionality from the one-dimensional diffusion to the three-dimensional interface reaction.

The Avrami-Erofeev equation in many cases provides a successful fitting of the experimental kinetic curves. This also defines the mechanism governing the process refined by the formal fitting of the reaction order *n*. However, defining an actual mechanism is often complicated and not a straightforward process. Particular difficulties are caused by *n* frequently changing (sometimes within a broad range) even when performing a series of similar experiments.

As an example, studies of MgH_2 hydrolysis in NH_4Cl solutions show different trends at low and at high concentrations of NH_4Cl. At low concentrations of NH_4Cl one-dimensional diffusion being the predominant mechanism. A three three-dimensional diffusion predominates, however, at high solution concentrations becoming the governing mechanism of the interaction [27].

For the hydrolysis of $(Ca,Mg)H_2$ [42], studies of the effect of various types of chlorides containing different types of cations, Na^+, Ca^{2+}, Mg^{2+} and NH_4^+, also showed that the hydrolysis reaction rate at low temperatures down to −20 °C is significantly boosted by the presence of Mg^{2+} and NH_4^+ ions in their chloride solutions.

We, however, in this study developed a different approach to modelling the kinetics of the MgH_2 hydrolysis process, which appears to be universally applicable to every case studied.

We have developed a model, in a previous study [43], that describes the kinetics of MgH_2 hydrolysis in pure water (see SI, Chapter S4). This model is based on the suggestion that the hydrolysis can be described by a pseudo-homogenous system, assuming that all the components of the interacting system are soluble and present in a solution. It is also based on the suggestion that all chemical reactions that take place are accounted for, including interaction of MgH_2 with hydrogen ions, formation of Mg^{2+} ions and Mg hydroxide $Mg(OH)_2$ and blocking of the MgH_2 surface by $Mg(OH)_2$ via the formation of the inactive reaction product. Such a model, even though it uses a simplified pseudo-homogenous approximation, satisfactorily describes both the kinetics of hydrogen evolution and changes of the pH of the solution during the interaction.

The use of such a model to describe the hydrolysis of MgH_2 in the presence of promoting additives is, unfortunately, quite complicated. We therefore propose the use of a simplified kinetics scheme to describe the kinetics of MgH_2 hydrolysis in the $MgCl_2$ solutions, based on the following assumptions.

Only the initial stages of the process show rapid changes (quick increase in the pH of the reaction mixture, see Fig. 6 for details). The pH values required to initiate the sedimentation of $Mg(OH)_2$ are therefore reached in the early stages of the hydrolysis, at a conversion level of just 0.04–1%. The pH of the solution quickly stabilizes after the start of $Mg(OH)_2$ sedimentation, the concentration of H^+ ions in the solution becoming stable, concentration being accounted for when determining the rate constants of different contributing reactions. Changes in pH at the beginning of the hydrolysis process will not, however, significantly affect the process of kinetic curve optimization. We therefore will not focus on the description of this hydrolysis process stage.

An overall kinetics scheme therefore includes three individual Reactions VI.1–VI.3. These elementary processes are:

$$S \rightarrow 2H_2\uparrow \quad \text{(VI.1)}$$

$$S \rightarrow P \quad \text{(VI.2)}$$

$$P \rightarrow 2H_2\uparrow \quad \text{(VI.3)}$$

(1) Fast interaction of solid MgH_2 (S) with water, releasing H_2. $MgH_2+2H_2O=Mg(OH)_2+2H_2$. k_1-rate constant of the process.
(2) $Mg(OH)_2$ formed during the hydrolysis process is in proportion to the amount of reacted MgH_2. The magnesium hydroxide (P) blocks the surface of the remaining MgH_2. k_2-rate constant of the process.
(3) Water molecules can still, despite the surface being blocked by $Mg(OH)_2$, slowly diffuse through the layer, so reaching and reacting with MgH_2, releasing hydrogen gas. k_3-rate constant of the process.

The reaction rates can be described by the following set of differential equations:

$$\frac{dH_2}{dt} = 2k_1S + 2k_3P \quad \text{(VII.1)}$$

$$\frac{dS}{dt} = -k_1S - k_2S \quad \text{(VII.2)}$$

$$\frac{dP}{dt} = k_2S - k_3P \quad \text{(VII.3)}$$

We note that pseudo elementary Reactions VII.1–VII.3 are monomolecular processes. Their reaction rate constants therefore have a dimensionality $[(\text{time})^{-1}]$. The kinetic curves can therefore be fitted using the rate of conversion $(V_t\ (H_2)/V_{theor}\ (H_2))$ instead of using reacting component concentrations. Initial concentration of MgH_2 is assumed to be 1 during such concentration fitting, the sum of concentrations $S + P + H_2$ at any moment of the process being equal to unity.

Refinements of the kinetics curves for MgH_2 hydrolysis, that give the values of the rate constants for the reactions, were performed using COPASI software [44].

We were able, using the described kinetic model, to satisfactorily describe experimental curves, as evidenced by Fig. 8.

The rate constants of the studied reactions at the same time, and as expected, show a dependence on the $MgCl_2$ content, as shown by the data listed in Table 4 and the graphs presented in Fig. 9.

Such observed dependencies can be summarized as follows:

(1) A slight increase in the rate constant k_1 with increasing $MgCl_2$ concentration, which can be due to changes in solution acidity;
(2) A decreasing k_2 with increasing $MgCl_2$ concentration. This can be related to a decrease in the number of $Mg(OH)_2$ blocking particles at the interface between the solution and the surface of MgH_2, resulting in reduced MgH_2 passivation;

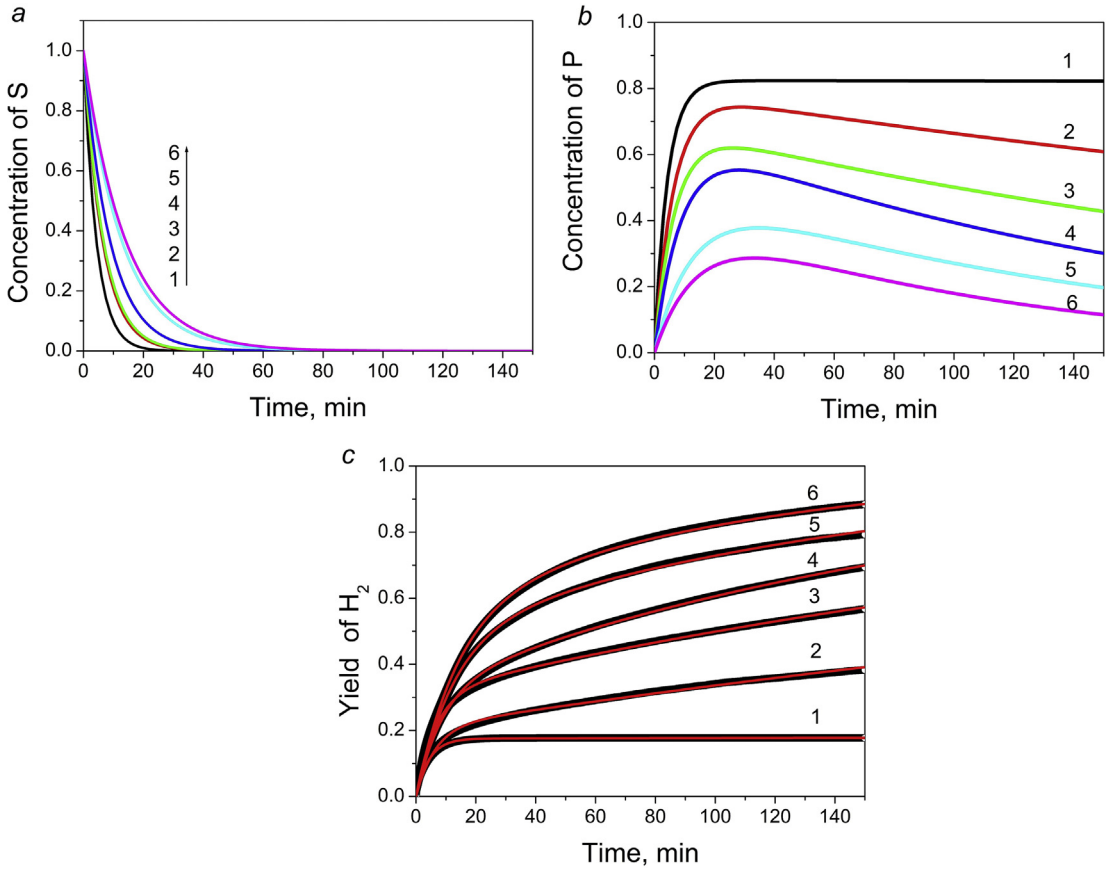

Fig. 8 – Time dependencies of concentrations of MgH_2 – S (*a*); $Mg(OH)_2$ – P (*b*); and H_2 yield – (*c*) for the different $MgCl_2$ solutions; 1–0; 2–0.0046; 3–0.0092; 4–0.0184; 5–0.0368; 6–0.0738 mol/L. Points are the experimental data and lines are the fitted curves.

Table 4 – Dependence of the refined model rate constants of MgH_2 hydrolysis on $MgCl_2$ concentration.

$[MgCl_2]$, mol/L	Rate constants, min^{-1}		
	k_1	k_2	k_3
0	0.031 ± 0.004	0.19 ± 0.02	0.000015 ± 0.0000003
0.0046	0.034 ± 0.003	0.12 ± 0.01	0.0017 ± 0.0004
0.0092	0.036 ± 0.004	0.10 ± 0.02	0.0031 ± 0.0004
0.0138	0.038 ± 0.002	0.07 ± 0.02	0.0048 ± 0.0007
0.0184	0.040 ± 0.002	0.07 ± 0.03	0.0054 ± 0.0008
0.0368	0.041 ± 0.002	0.037 ± 0.006	0.0064 ± 0.0009
0.0738	0.043 ± 0.002	0.021 ± 0.004	0.009 ± 0.001

(3) A more distinct increase in k_3 than k_1 as $MgCl_2$ concentration increases. This is not only associated with changes in solution pH, but also and primarily with the growth in the size of the $Mg(OH)_2$ crystallites and the corresponding higher rate of water diffusion through the inhomogeneous passivating film (see Chapter 3.6 and Figs. 6 and 7).

This explanation of the promoting action of different metal chlorides during the MgH_2 hydrolysis reaction describes, despite its simplicity, the observed experimental dependencies well and is expected to be developed further in the future.

Recently hydrolysis of magnesium-based materials, including alloys, composites and hydrides, has become a subject of a growing interest and resulted in numerous publications. These included review papers [45–47] and research publications focusing on the effects of various additives - LaH_3 and Ni [48], Si [49] and aluminium, graphite, $AlCl_3$, $MgCl_2$ [50] – on the hydrolysis process performed in aqueous solutions of $MgCl_2$ and NaCl.

Hydrolysis efficiency of magnesium hydride has been successfully improved by using various approaches. These were considered in a review paper [45] and included (a) use of prepared by ball milling composites of MgH_2 with catalyzing additives of oxides and sulfides; (b) utilizing micro-galvanic cells facilitating the electrochemical corrosion; (c) employing the solutions containing two types of anions, e.g. NO_3^- and CO_3^{2-}. The additives of halides – chlorides and fluorides – allowed to tune the composition of the solution during the hydrolysis of Mg-containing materials to increase the rates and yield of the hydrolysis.

Furthermore, introduction of alkali and alkali-earth metals has proved to be an efficient way to significantly enhance the

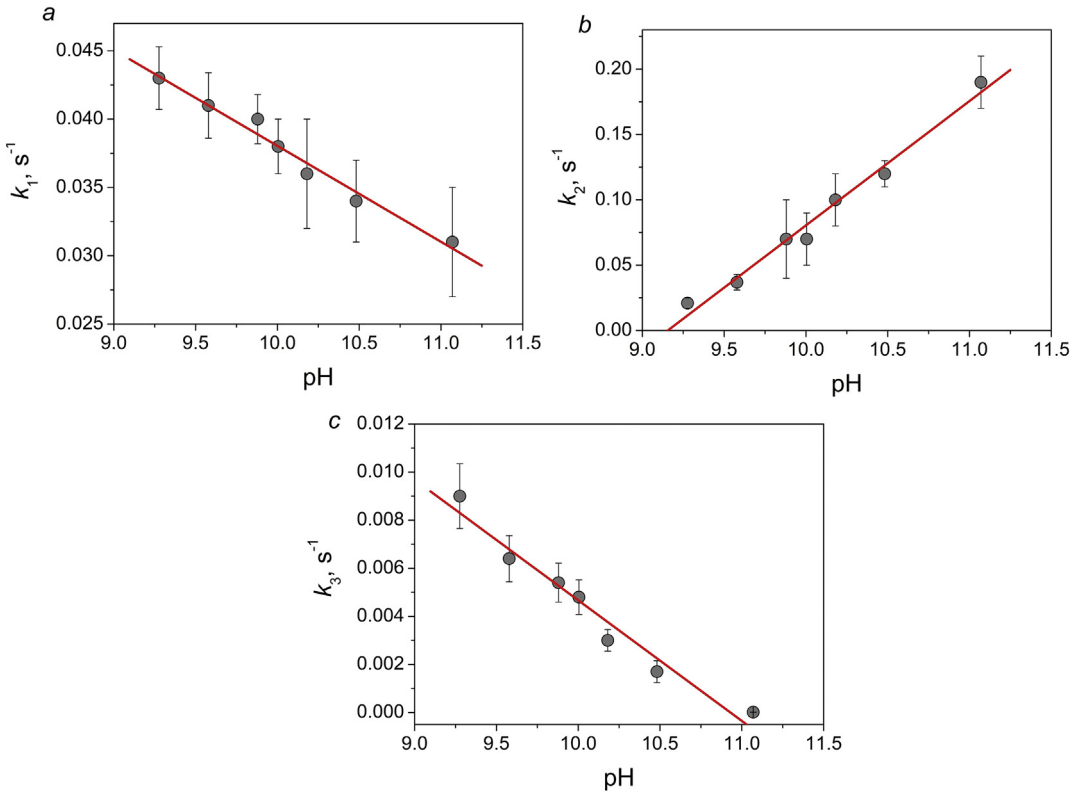

Fig. 9 – Dependencies of the reaction rate constants, k_1 (a); k_2 (b) and k_3 (c) for the hydrolysis process on the pH of the solutions.

hydrogen generation performance due to their higher reactivity towards water than that of Mg [46]. At the same time, introduction of transition metals and/or rare earth metals increased the corrosion potential difference between them and Mg or their hydrides and resulted in the formation of the micro-galvanic cells effectively promoting the hydrolysis reaction of Mg-rich phases and thus showing enhanced hydrogen generation efficiency [46].

A key aspect in achieving an advanced hydrolysis performance of magnesium hydride in the solutions of chlorides appears to be in affecting the properties of the surface hydroxide layer covering the hydride by making it permeable for water. This may happen in different ways, including: (a) Decrease in activation energy of the inhibition of the formation of the passivation layer as in the solutions of $CoCl_2$ [51]; (b) Changes in the surface tension value by using various surfactants, which creates a developed network of the channels suitable for the efficient diffusion of water to the surface of MgH_2 [52]; (c) Nanostructuring of magnesium containing materials by reactive ball milling in hydrogen gas or by adding during the milling additives of graphite and nickel favoring formation of the well developed and active surface area with increased activity which is suitable for a quick hydrolysis process in the solutions of $MgCl_2$ [53] or NaCl and NH_4Cl [54].

In contrast, when the oxide/hydroxide layer is dense and poorly permeable for water, this slaws down/stops the hydrolysis process as for the $Mg_{17}Al_{12}$ alloy, decreasing the yield of the hydrolysis process even if various promoters of the hydrolysis are added to the alloy during its milling (graphite, $AlCl_3$, $MgCl_2$).

Altogether these studies were aimed at a development of the cost efficient, easy to scale up systems to be used in the hydrolysis process and demonstrated a significant progress in the field.

However, elaboration of the model description of the kinetics of the hydrolysis process, particularly when beneficially influenced by chlorides – has not been properly addressed before our present study. Thus, the outcome of this work which proposed and verified the model describing the kinetics of hydrogen generation in $MgCl_2$ solutions is a significant step forward in further advancements towards the use of magnesium based materials in the hydrolysis process.

Conclusions

The role of different chloride salts as catalytic additives is, despite a clear influence of aqueous solution pH upon MgH_2 hydrolysis which affects the reaction kinetics and yield of hydrogen, not yet completely understood. This problem is therefore addressed in this work. The addition of $MgCl_2$ salt

promotes the hydrolysis reaction with clear rate and yield advantages compared with the other chlorides.

The MgH_2 hydrolysis reaction in the $MgCl_2$ solutions was investigated at pseudo-isothermal conditions. Based on the analysis of the process kinetics, our conclusions for changes of solution pH and the characterization of the phase-structural composition of the products are as follows:

- The addition of small amounts (17/100 wt parts) of $MgCl_2$ leads to a factor of ~4 increase in the yield of the hydrolysis reaction, a factor of ~1 decrease in the pH of the working solution and an increase in the hydrolysis product - $Mg(OH)_2$ - precipitate crystallinity.
- pH of a working solution and conversion of the MgH_2 hydrolysis reaction linearly depend on the logarithm of $MgCl_2$ concentration.
- pH of the reaction mixture in the presence of $MgCl_2$ is well described by considering a system "weak base and its salt with strong acid" type buffer solution.
- The mechanism of MgH_2 hydrolysis in $MgCl_2$ solutions includes the formation of the buffer solution that controls the pH of the reaction mixture. This leads to a decreasing supersaturation coefficient for the solution by $Mg(OH)_2$ and corresponding increase in the size of the critical nuclei and crystallinity of the precipitates. This is followed by the formation of an inhomogeneous passivation film at the surface of MgH_2.
- A mechanism and a kinetics model for the MgH_2 hydrolysis process in water solutions, that can successfully describe the experimental data, have been proposed. The process involves the hydrolysis reaction, the resulting generation of hydrogen and the formation of $Mg(OH)_2$. It, however, also involves passivation of the MgH_2 surface by the $Mg(OH)_2$ precipitate, followed by re-passivation. The rate constants for these processes were defined. An increase in $MgCl_2$ concentration leads to just a minor increase in the rate constant for MgH_2 interaction with water. It, however, also leads to a sharp increase in the rate constant for the re-passivation of the MgH_2 surface. This agrees well with XRD studies of the precipitates, which show the formation of well crystallized $Mg(OH)_2$, this causing the formation of an inhomogeneous passivation film on the MgH_2 surface and improving water access to MgH_2.

Declaration of competing interest

The authors declare that they have no known competing financial interests or personal relationships that could have appeared to influence the work reported in this paper.

Acknowledgements

This work has received support from the NATO SPS project G5233 Portable Energy Supply.

We thank Dr. R.V. Denys (IFE and HYSTORSYS) for his help in the evaluation of the XRD data.

Appendix A. Supplementary data

Supplementary data to this article can be found online at https://doi.org/10.1016/j.ijhydene.2021.09.249.

REFERENCES

[1] Uyar TS, Beşikci D. Integration of hydrogen energy systems into renewable energy systems for better design of 100% renewable energy communities. Int J Hydrogen Energy 2017;42(4):2453–6. https://doi.org/10.1016/j.ijhydene.2016.09.086.

[2] Teichmann D, Arlt W, Wasserscheid P, Freymann R. A future energy supply based on liquid organic hydrogen carriers (LOHC). Energy Environ Sci 2011;4(8):2767–73. https://doi.org/10.1039/C1EE01454D.

[3] Momirlan M, Veziroglu TN. Current status of hydrogen energy. Renew Sustain Energy Rev 2002;6(1–2):141–79. https://doi.org/10.1016/S1364-0321(02)00004-7.

[4] Wilberforce T, Alaswad A, Palumbo A, Dassisti M, Olabi AG. Advances in stationary and portable fuel cell applications. Int J Hydrogen Energy 2016;41(37):16509–22. https://doi.org/10.1016/j.ijhydene.2016.02.057.

[5] Liu BH, Li ZP. A review: hydrogen generation from borohydride hydrolysis reaction. J Power Sources 2009;187(2):527–34. https://doi.org/10.1016/j.jpowsour.2008.11.032.

[6] Marrero-Alfonso EY, Beaird AM, Davis TA, Matthews MA. Hydrogen generation from chemical hydrides. Ind Eng Chem Res 2009;48(8):3703–12. https://doi.org/10.1021/ie8016225.

[7] Kushch SD, Kuyunko NS, Nazarov RS, Tarasov BP. Hydrogen-generating compositions based on magnesium. Int J Hydrogen Energy 2011;36(1):1321–5. https://doi.org/10.1016/j.ijhydene.2010.06.115.

[8] Czech E, Troczynski T. Hydrogen generation through massive corrosion of deformed aluminum in water. Int J Hydrogen Energy 2010;35(3):1029–37. https://doi.org/10.1016/j.ijhydene.2009.11.085.

[9] Wang HZ, Leung DY, Leung MKH, Ni M. A review on hydrogen production using aluminum and aluminum alloys. Renew Sustain Energy Rev 2009;13(4):845–53. https://doi.org/10.1016/j.rser.2008.02.009.

[10] Zou MS, Guo XY, Huang HT, Yang RJ, Zhang P. Preparation and characterization of hydro-reactive Mg–Al mechanical alloy materials for hydrogen production in seawater. J Power Sources 2012;219:60–4. https://doi.org/10.1016/j.jpowsour.2012.07.008.

[11] Ma M, Ouyang L, Liu J, Wang H, Shao H, Zhu M. Air-stable hydrogen generation materials and enhanced hydrolysis performance of MgH_2-$LiNH_2$ composites. J Power Sources 2017;359:427–34. https://doi.org/10.1016/j.jpowsour.2017.05.087.

[12] Hiraki T, Hiroi S, Akashi T, Okinaka N, Akiyama T. Chemical equilibrium analysis for hydrolysis of magnesium hydride to generate hydrogen. Int J Hydrogen Energy 2012;37(17):12114–9. https://doi.org/10.1016/j.ijhydene.2012.06.012.

[13] Tayeh T, Awad AS, Nakhl M, ZakhourM, Silvain JF, Bobet JL. Production of hydrogen from magnesium hydrides hydrolysis. Int J Hydrogen Energy 2014;39(7):3109–17. https://doi.org/10.1016/j.ijhydene.2013.12.082.

[14] Chao CH, Jen TC. Reaction of magnesium hydride with water to produce hydrogen. Appl Mech Mater 2013;302:151–7. https://doi.org/10.4028/www.scientific.net/AMM.302.151.

[15] Verbovytskyy YuV, Berezovets VV, Kytsya AR, Zavaliy IYu, Yartys VA. Hydrogen generation by hydrolysis of MgH_2. Mater Sci 2020;56:1–14. https://doi.org/10.1007/s11003-020-00390-5.

[16] Grosjean M-H, Zidoune M, Roué L. Hydrogen production from highly corroding Mg-based materials elaborated by ball

milling. J Alloys Compd 2005;404–406:712–5. https://doi.org/10.1016/j.jallcom.2004.10.098.
[17] Grosjean M-H, Zidoune M, Roué L, Huot J-Y. Hydrogen production via hydrolysis reaction from ball-milled Mg-based materials. Int J Hydrogen Energy 2006;31:109–19. https://doi.org/10.1016/j.ijhydene.2005.01.001.
[18] Makhaev VD, Petrova LA, Tarasov BP. Hydrolysis of magnesium hydride in the presence of ammonium salts. Russ J Inorg Chem 2008;53(6):858–60. https://doi.org/10.1134/S0036023608060077.
[19] Grosjean MH, Roué L. Hydrolysis of Mg–salt and MgH_2–salt mixtures prepared by ball milling for hydrogen production. J Alloys Compd 2006;416:296–302. https://doi.org/10.1016/j.jallcom.2005.09.008.
[20] Tegel M, Schöne S, Kieback B, Röntzsch L. An efficient hydrolysis of MgH_2-based materials. Int J Hydrogen Energy 2017;42(4):2167–76. https://doi.org/10.1016/j.ijhydene.2016.09.084.
[21] Li S, Gan DY, Zhu YF, Liu YN, Zhang G, Li LQ. Influence of chloride salts on hydrogen generation via hydrolysis of MgH2 prepared by hydriding combustion synthesis and mechanical milling. Trans Nonferrous Metals Soc China 2017;27:562–8. https://doi.org/10.1016/S1003-6326(17)60062-1.
[22] Zhao Z, Zhu Y, Li L. Efficient catalysis by $MgCl_2$ in hydrogen generation via hydrolysis of Mg-based hydride prepared by hydriding combustion synthesis. Chem Commun 2012;48(44):5509–11. https://doi.org/10.1039/c2cc32353b.
[23] Ouyang L, Ma M, Huang M, Duan R, Wang H, Sun L, Zhu M. Enhanced hydrogen generation properties of MgH_2-based hydrides by breaking the magnesium hydroxide passivation layer. Energies 2015;8(5):4237–52. https://doi.org/10.3390/en8054237.
[24] Sevastyanova LG, Klyamkin SN, Bulychev BM. Generation of hydrogen from magnesium hydride oxidation in water in presence of halides. Int J Hydrogen Energy 2020;45:3046–52. https://doi.org/10.1016/j.ijhydene.2019.11.226.
[25] Sevastyanova LG, Genchel VK, Klyamkin SN, Larionova PA, Bulychev BM. Hydrogen generation by oxidation of "mechanicalalloys" of magnesium with iron and copper in aqueous salt solutions. Int J Hydrogen Energy 2017;42:16961–7. https://doi.org/10.1016/j.ijhydene.2017.05.242.
[26] Gan D, Liu Y, Zhang J, Zhang Y, Cao C, Zhu Y, Li L. Kinetic performance of hydrogen generation enhanced by $AlCl_3$ via hydrolysis of MgH_2 prepared by hydriding combustion synthesis. Int J Hydrogen Energy 2018;43:10232–9. https://doi.org/10.1016/j.ijhydene.2018.04.119.
[27] Huang M, Ouyang L, Wang H, Liu J, Zhu M. Hydrogen generation by hydrolysis of MgH_2 and enhanced kinetics performance of ammonium chloride introducing. Int J Hydrogen Energy 2015;40(18):6145–50. https://doi.org/10.1016/j.ijhydene.2015.03.058.
[28] Chen J, Fu H, Xiong Y, Xu J, Zheng J, Li X. $MgCl_2$ promoted hydrolysis of MgH_2 nanoparticles for highly efficient H_2 generation. Nanomater Energy 2014;10:337–43. https://doi.org/10.1016/j.nanoen.2014.10.002.
[29] Rietveld HM. A profile refinement method for nuclear and magnetic structures. J Appl Crystallogr 1969;2(2):65–71. https://doi.org/10.1107/S0021889869006558.
[30] Toby BH, Von Dreele RB. GSAS-II: the genesis of a modern open-source all purpose crystallography software package. J Appl Crystallogr 2013;46(2):544–9. https://doi.org/10.1107/S0021889813003531.
[31] Denys RV, Riabov AB, Maehlen JP, Lototsky MV, Solberg JK, Yartys VA. In situ synchrotron X-ray diffraction studies of hydrogen desorption and absorption properties of Mg and Mg–Mm–Ni after reactive ball milling in hydrogen. Acta Mater 2009;57(13):3989–4000. https://doi.org/10.1016/j.actamat.2009.05.004.
[32] Pannach M, Bette S, Freyer D. Solubility equilibria in the system $Mg(OH)_2$–$MgCl_2$–H_2O from 298 to 393 K. J Chem Eng Data 2017;62(4):1384–96. https://doi.org/10.1021/acs.jced.6b00928.
[33] Newman ES. A study of the system magnesium oxide-magnesium chloride-water and the heat of formation of magnesium oxychloride. J Res Natl Bur Stand 1955;54(6):347–55. https://doi.org/10.6028/jres.054.039.
[34] Urwongse L, Sorrell CA. The system MgO-$MgCl_2$-H_2O at 23 °C. J Am Ceram Soc 1980;63(9-10):501–4. https://doi.org/10.1111/j.1151-2916.1980.tb10752.x.
[35] Sorrell CA, Armstrong CR. Reactions and equilibria in magnesium oxychloride cements. J Am Ceram Soc 1976;59(1-2):51–4. https://doi.org/10.1111/j.1151-2916.1976.tb09387.x.
[36] Dinnebier RE, Halasz I, Freyer D, Hanson JC. The crystal structures of two anhydrous magnesium hydroxychloride phases from in situ synchrotron powder diffraction data. Z Anorg Allg Chem 2011;637(11):1458–62. https://doi.org/10.1002/zaac.201100139.
[37] Lurie YY. Handbook on analytical chemistry. Moscow: Chemistry; 1971 (In Russian).
[38] Klein DH, Smith MD, Driy JA. Homogeneous nucleation of magnesium hydroxide. Talanta 1967;14(8):937–40. https://doi.org/10.1016/0039-9140(67)80126-7.
[39] Farkas L. Keimbildungsgeschwindigkeit in übersättigten Dämpfen. Z Phys Chem 1927;125(1):236–42. https://doi.org/10.11588/heidok.00013220.
[40] LaMer VK, Dinegar RH. Theory, production and mechanism of formation of monodispersed hydrosols. J Am Chem Soc 1950;72(11):4847–54. https://doi.org/10.1021/ja01167a001.
[41] Sugimoto T. Preparation of monodispersed colloidal particles. Adv Colloid Interface Sci 1987;28:65–108. https://doi.org/10.1016/0001-8686(87)80009-x.
[42] Zhong S, Wu C, Li J, Chen Y, Wang Y, Yan Y. Effect of cations in chloride solutions on low-temperature hydrolysis performances and mechanisms of Mg–Ca-based hydride. J Alloys Compd 2021;851:156762. https://doi.org/10.1016/j.jallcom.2020.156762.
[43] Kytsya A, Berezovets V, Verbovytskyy Yu, Zavaliy I, Yartys V. Modeling of kinetics of MgH_2 hydrolysis. In: XVII scientific conference "Lviv chemical readings – 2019", Lviv, Ukraine; 02–05 June, 2019. – M3.
[44] Hoops S, Sahle S, Gauges R, Lee C, Pahle J, Simus N, Singhal M, Xu L, Mendes P, Kummer U. COPASI—a complex pathway simulator. Bioinformatics 2006;22(24):3067–74. https://doi.org/10.1093/bioinformatics/btl485.
[45] Xie XiuBo, Cui Ni, Wang Baolei, Zhang Yuping, Zhao Xiangjin, Liu Li, Wang Bing, Du Wei. Recent advances in hydrogen generation process via hydrolysis of Mg based materials: a short review. J Alloys Compd 2020;816:152634. https://doi.org/10.1016/j.jallcom.2019.152634.
[46] Liu Zipeng, Zhong Jinling, Leng Haiyan, Xia Guanglin, Yu Xuebin. Hydrolysis of Mg-based alloys and their hydrides for efficient hydrogen generation. Int J Hydrogen Energy 2021;46:18988–9000. https://doi.org/10.1016/j.ijhydene.2021.03.063.
[47] Liu Z, Zhong J, Leng H, Xia G, Yu X. Hydrolysis of Mg-based alloys and their hydrides for efficient hydrogen generation. Int J Hydrogen Energy 2021;46:18988–9000. https://doi.org/10.1016/j.ijhydene.2021.03.063.
[48] Zhong H, Wang H, Liu JW, Sun DL, Fang F, Zhang QA, Ouyang LZ, Zhu M. Enhanced hydrolysis properties and energy efficiency of MgH_2-base hydrides. J Alloys Compd 2016;680:419–26. https://doi.org/10.1016/j.jallcom.2016.04.148.
[49] Tan Z, Ouyang L, Liu J, Wang H, Shao H, Zhu M. Hydrogen generation by hydrolysis of Mg-Mg_2Si composite and

enhanced kinetics performance from introducing of $MgCl_2$ and Si. Int J Hydrogen Energy 2018;43:2903–12. https://doi.org/10.1016/j.ijhydene.2017.12.163.

[50] Al Bacha S, Zakhour M, Nakhl M, Bobet J-L. Effect of ball milling in presence of additives (graphite, $AlCl_3$, $MgCl_2$ and NaCl) on the hydrolysis performances of $Mg_{17}Al_{12}$. Int J Hydrogen Energy 2020;45:6102–9. https://doi.org/10.1016/j.ijhydene.2019.12.162.

[51] Coskuner Filiz B. Investigation of the reaction mechanism of the hydrolysis of MgH_2 in $CoCl_2$ solutions under various kinetic conditions. React Kinet Mech Catal 2021;132:93–109. https://doi.org/10.1007/s11144-020-01923-4.

[52] Chen Y, Wang M, Guan F, Yu R, Zhang Y, Qin H, Chen X, Fu Q, Wang Z. Study on hydrolysis of magnesium hydride by interface control. Int J Photoenergy 2020;2020:8859770. https://doi.org/10.1155/2020/8859770.

[53] Pighin SA, Urretavizcaya G, Bobet J-L, Castro FJ. Nanostructured Mg for hydrogen production by hydrolysis obtained by MgH_2 milling and dehydriding. J Alloys Compd 2020;827:154000. https://doi.org/10.1016/j.jallcom.2020.154000.

[54] Al Bacha S, Thienpont A, Zakhour M, Nakhl M, Bobet J-L. Clean hydrogen production by the hydrolysis of magnesium-based material: effect of the hydrolysis solution. J Clean Prod 2021;282:124498. https://doi.org/10.1016/j.jclepro.2020.124498.